Naval Research Laboratory
Stennis Space Center, MS 39529-5004

NRL/FR/7320--01-9976

Evaluation of an Application of Adjoint Methods to Yellow Sea Modeling

CATHERINE R. EDWARDS
CHERYL ANN BLAIN

Ocean Dynamics and Prediction Branch
Oceanography Division

September 4, 2001

REPORT DOCUMENTATION PAGE

Form Approved
OMB No. 0704-0188

1. REPORT DATE *(DD-MM-YYYY)*	2. REPORT TYPE	3. DATES COVERED *(From - To)*
September 4, 2001	Formal	August 1999-August 2000

4. TITLE AND SUBTITLE

Evaluation of an Application of Adjoint Methods to Yellow Sea Modeling

5a. CONTRACT NUMBER

5b. GRANT NUMBER

5c. PROGRAM ELEMENT NUMBER
PE - 0602435N

6. AUTHOR(S)

Catherine R. Edwards and Cheryl Ann Blain

5d. PROJECT NUMBER

5e. TASK NUMBER

5f. WORK UNIT NUMBER

7. PERFORMING ORGANIZATION NAME(S) AND ADDRESS(ES)

Naval Research Laboratory
Oceanography Division
Stennis Space Center, MS 39529-5004

8. PERFORMING ORGANIZATION REPORT NUMBER

NRL/FR/7320--01-9976

9. SPONSORING / MONITORING AGENCY NAME(S) AND ADDRESS(ES)

Naval Research Laboratory
4555 Overlook Ave., SW
Washington, DC 20375-5320

10. SPONSOR / MONITOR'S ACRONYM(S)

11. SPONSOR / MONITOR'S REPORT NUMBER(S)

12. DISTRIBUTION / AVAILABILITY STATEMENT

Approved for public release; distribution is unlimited.

13. SUPPLEMENTARY NOTES

14. ABSTRACT

In the application of adjoint methods, adjoint model equations are used to compute the directions in which unknown model parameters should be adjusted to achieve an optimal fit between modeled dynamics and observations. Many researchers have successfully applied an incremental adjoint modeling approach to infer open ocean boundary forcing that accounts for available observations.

In this study, an adjoint model system, comprising a simple model and its inverse in conjuction with a more complex forward model, is applied in the Yellow Sea to predict tidal elevations and currents throughout the region using the incremental approach. The nonlinear finite element model ADCIRC-2DDI is used as the complex forward model with the linear finite difference adjoint model of Thompson in the inverse assimilative loop. Field measurements include sea surface elevations derived from altimeter data and tidal stations, and currents from three ADCP locations.

Various implementations of the feedback between the linear inverse model and the nonlinear forward model are examined. Comparisons between large domain solutions without data assimilation and limited area domains forced with adjoint model predictions on the open boundary form the basis for evaluation of the approach. Incompatibilities in model discretization, resolution, and boundary condition formulation severely limit the advantages of the application of the incremental approach using the finite difference adjoint model of Thompson as implemented here.

15. SUBJECT TERMS

Data assimilation, adjoint methods, incremental approach, Yellow Sea modeling, finite element models

16. SECURITY CLASSIFICATION OF:			17. LIMITATION OF ABSTRACT	18. NUMBER OF PAGES	19a. NAME OF RESPONSIBLE PERSON
a. REPORT	b. ABSTRACT	c. THIS PAGE			Cheryl Ann Blain
Unclassified	Unclassified	Unclassified	UL	34	19b. TELEPHONE NUMBER *(include area code)* 228-688-5450

Standard Form 298 (Rev. 8-98)
Prescribed by ANSI Std. Z39.18

CONTENTS

EVALUATION OF AN APPLICATION OF ADJOINT METHODS TO YELLOW SEA MODELING

1. INTRODUCTION

Adjoint methods, used for over a decade in the field of meteorology, have provided a powerful tool to ocean modelers as field observations are more readily available and data assimilation becomes more computationally possible. The evolution and review of some applications of adjoints and other assimilative methods can be found in Ghil and Manalotte-Rizzoli (1991) and Ghil et al. (1997).

Several recent studies have applied adjoint methods to infer open boundary forcings from assimilated data (Seiler 1993; Lardner 1993; Thompson and Griffin 1998). The incremental approach (Thompson et al. 1998; Courtier et al. 1994; Thompson et al. 2000) involves a straightforward modification of the Gauss-Newton algorithm commonly used for iteratively solving nonlinear regression problems. The adjoint of a dynamically simple forward model is calculated and the cost function associated with point data is minimized given station elevation and velocity information. Further iterated with a dynamically complex ocean model, this approach can provide even more accurate ocean predictions relative to the observed state.

Adjoint methods that derive open boundary forcing can also facilitate limited area modeling. Limited area domains have the advantages of reducing computation time or allowing even greater refinement in nearshore waters. Traditionally, though, this approach has its shortcomings in both theoretical and practical aspects. Blain et al. (1994), in a study of the effect of domain size on computed storm surge response, found that domain size and the placement of the open ocean boundaries have a direct effect on the resulting solution. Dynamics generated within a larger area domain often cannot be captured within a limited area domain or specified through the open boundary forcing of limited area domains. A practical advantage of large area domains has been that their boundaries extend far enough offshore that boundary forcing can be interpolated from larger global solutions. Open boundaries of limited area domains lie well nearshore of "proven" global solutions; thus, finding appropriate open boundary forcing can become problematic. Adjoint methods may surpass such limitations to provide appropriate boundary forcing for limited area domains.

Manuscript approved September 25, 2000.

For this study, the complex forward model is defined by a nonlinear finite element model, ADCIRC. Perhaps the greatest advantage of finite element discretizations over more traditional finite difference methods is the ability to vary resolution over the domain, more accurately representing the coastal boundary and increasing resolution in shallower waters. In this manner, use of complicated nested or multiresolution finite difference grids can be avoided while improving the solution in nearshore regions and greatly reducing overall computation time. An available adjoint model system of Thompson (Griffin and Thompson 1996; Thompson and Griffin 1998; Pistek et al. 1998) is selected as the data-assimilative component.

The question arises as to whether an advantage can be gained by applying the incremental approach to a complex forward model whose adjoint model system is not strictly an adjoint of the forward model. Certainly, success of this approach would be appealing, eliminating the need to develop a separate adjoint for each forward model. In this study, the possible applications of finite difference-based adjoint methods in conjunction with finite element-based models are investigated in the Yellow Sea. Specifically, feasibility of the incremental approach is explored, using the nonlinear finite element model ADCIRC as the complex forward model and the linear finite difference adjoint model of Thompson (ADJOINT) in the linear inverse model loop with data assimilation. Also examined is the degree to which linear adjoint methods can provide more accurate open boundary forcing for nonlinear forward models applied over limited area domains external to the data assimilative loop. After discussing the specifics of the model system, the report presents the finite element grids and observational station data used in the model system. The later sections describe and analyze the implementation of both non-assimilative and assimilative experiments and present conclusions.

2. MODEL SYSTEM

The incremental modeling approach involves two components. First, a dynamically simple model and its adjoint, in this case, the ADJOINT model of Thompson (Griffin and Thompson 1996; Thompson and Griffin 1998; Pistek et al. 1998), is used to assimilate data and compute optimal boundary forcings constrained by both the dynamical equations and observations. Secondly, a model which includes more complex nonlinear dynamics, ADCIRC (Luettich et al. 1992; Kolar et al. 1994a,b; Westerink et al. 1994a,b), serves as the complex forward model. The forward model uses open boundary forcing derived from the solution of linear ADJOINT model. Prediction errors in the complex forward model solution at observational stations are then assimilated into the linear model system to find the increment by which the controls, in this case, forcing on the complex model open boundary, are adjusted. This process involves repeated runs of the linear model and its adjoint to iteratively minimize the modified cost function, effectively giving a pair of nested iterations (Thompson et al. 2000). The modified cost function is essentially the difference between the complex model prediction and the data at the observational points. This approach is computationally efficient and simple, but has limitations. In particular,

if the simple model dynamics are not sufficiently close to the Jacobian of the complex model, there is no guarantee of convergence to the true state, or that the solution will converge at all (Thompson et al. 1998).

2.1 ADCIRC

The complex forward model computations are performed using the finite element-based ADCIRC-2DDI, the depth-integrated version of a set of two- and three-dimensional fully nonlinear hydrodynamic codes. ADCIRC-2DDI solves the two-dimensional, depth-integrated shallow water equations, subject to the hydrostatic pressure and Boussinesq approximations. For the applications discussed here, the baroclinic terms in the momentum conservation equations are neglected, leading to the following set of governing equations in the primitive, nonconservative form, using spherical coordinates:

$$\frac{\partial \zeta}{\partial t} + \frac{1}{R cos\phi}\frac{\partial\, UH}{\partial \lambda} + \frac{1}{R}\frac{\partial\, VH}{\partial \phi} - \frac{VH\, tan\phi}{R} = 0 \tag{1}$$

$$\frac{\partial U}{\partial t} + \frac{U}{R cos\phi}\frac{\partial U}{\partial \lambda} + \frac{V}{R}\frac{\partial U}{\partial \phi} - \left(\frac{U\, tan\phi}{R} + f\right)V = -\frac{1}{R cos\phi}\frac{\partial}{\partial \lambda}\Big[g\zeta - g(\eta + \Upsilon)\Big] - \frac{\tau_{b\lambda}}{\rho_o H} - \tau_* U \tag{2}$$

$$\frac{\partial V}{\partial t} + \frac{U}{R cos\phi}\frac{\partial V}{\partial \lambda} + \frac{V}{R}\frac{\partial V}{\partial \phi} + \left(\frac{U\, tan\phi}{R} + f\right)U = -\frac{1}{R}\frac{\partial}{\partial \phi}\Big[g\zeta - g(\eta + \Upsilon)\Big] - \frac{\tau_{b\phi}}{\rho_o H} - \tau_* V \tag{3}$$

where t is time, λ, ϕ are degrees longitude (east of Greenwich positive) and degrees latitude (north of the equator positive), ζ is free surface elevation (relative to the geoid), U, V are depth integrated horizontal velocities, and H is the total water column thickness. Ω is the angular speed of the Earth ($7.29212\text{x}10^{-5}$ rad/s), R the radius of the Earth, f ($= 2\Omega \sin\phi$) is the Coriolis parameter determined by latitude, g is gravity, and $(\eta + \Upsilon)$ represents the Newtonian tidal potential, earth tide, self attraction, and load tide term. Lastly, ρ_o is the reference density of water. Standard quadratic parameterizations for the bottom stresses $\tau_{b\lambda,\phi}$ are used:

$$\tau_{b\lambda} = C_f (U^2 + V^2)^{1/2} U \tag{4}$$

$$\tau_{b\phi} = C_f(U^2 + V^2)^{1/2}V, \tag{5}$$

where C_f is a dimensionless friction coefficient.

The Generalized Wave Continuity Equation is obtained by reformulating Eqs. (1) through (3) and is discretized in space using the finite element method (Lynch and Gray 1979; Lynch 1983; Kinnmark 1984; Westerink and Gray 1991) and, in time, using finite difference techniques. Further details of the ADCIRC family of codes are presented by Luettich et al. (1992), Kolar et al. (1994a,b), and Westerink et al. (1994a,b).

2.2 ADJOINT

In the application of adjoint methods, the adjoint of the discrete linear simple model equations is used to compute the directions in which unknown model parameters are adjusted to achieve a better fit of the modeled dynamics to observed values. The equations of motion used by the linear ADJOINT forward model are expressed in Cartesian coordinates as

$$\frac{\partial U}{\partial t} - fV + g\frac{\partial \zeta}{\partial x} = -\tau^{(B,x)} \tag{6}$$

$$\frac{\partial V}{\partial t} + fU + g\frac{\partial \zeta}{\partial y} = -\tau^{(B,y)} \tag{7}$$

$$\frac{\partial \zeta}{\partial t} + \frac{\partial (UH)}{\partial x} + \frac{\partial (VH)}{\partial y} = 0, \tag{8}$$

where the bottom stresses $\tau^{(B,x)}$ and $\tau^{(B,y)}$ are linear in U and V, respectively, with frictional coefficient κ. Due to widely varying bottom topography (mud flats to rocky terrain) in the Yellow Sea, the linear bottom friction coefficient κ is spatially varied according to five separate regimes over the domain (Fig. 1). The open boundary is forced with the following condition:

$$U_n = \sqrt{\frac{g}{h}}\zeta + \xi, \tag{9}$$

where h is the bathymetric water depth and the time-varying boundary forcing ξ is considered unknown in the linear forward model solution. This type of boundary condition allows transient waves generated inside the model domain to radiate away with minimal reflection (Thompson et al. 2000).

The unknown tidal amplitudes and phases at the open boundary ζ are estimated from assimilated interior station data (Fig. 2), and the solution of the shallow water equations is posed as a boundary value problem in the frequency domain. The estimation procedure is based on a

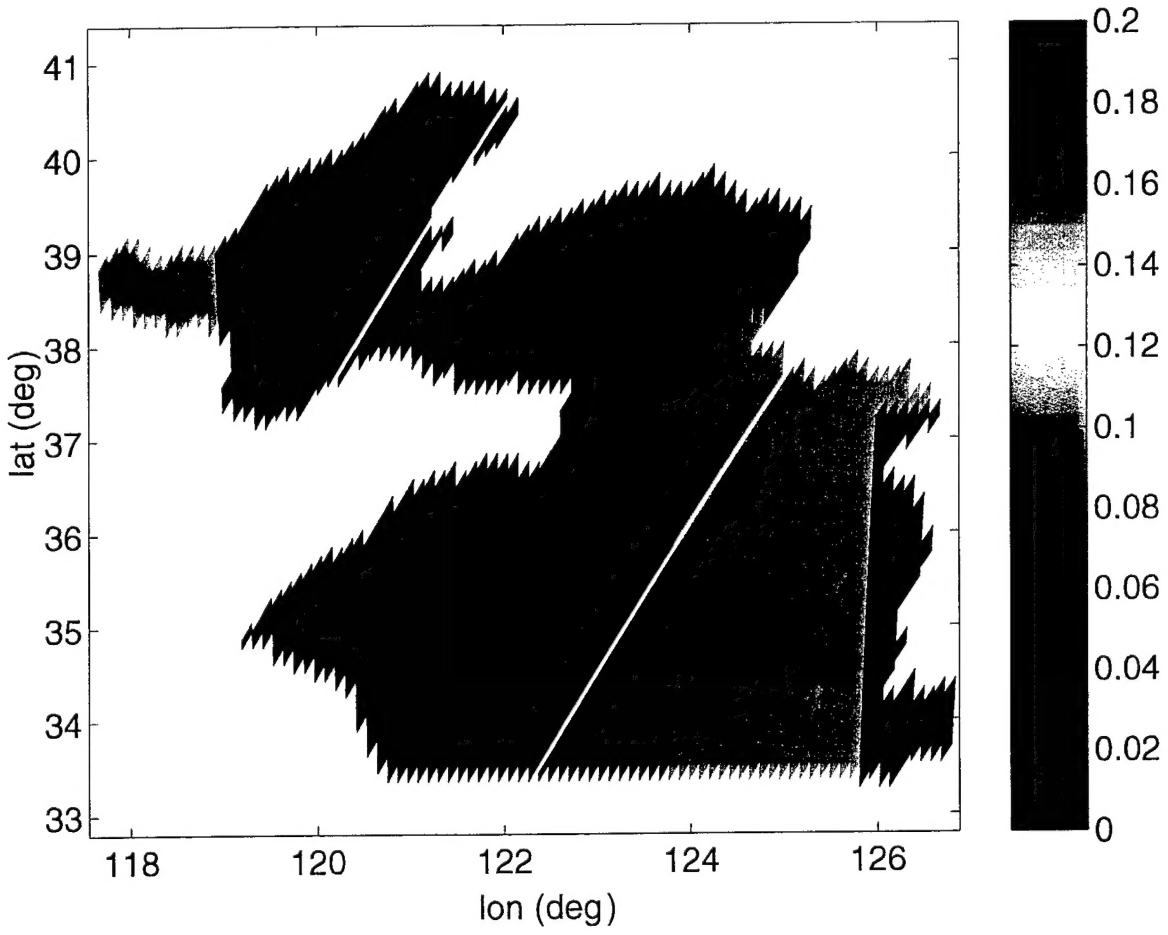

Fig. 1 — Dimensionless linear drag coefficient κ used by the linear ADJOINT model in the Yellow Sea

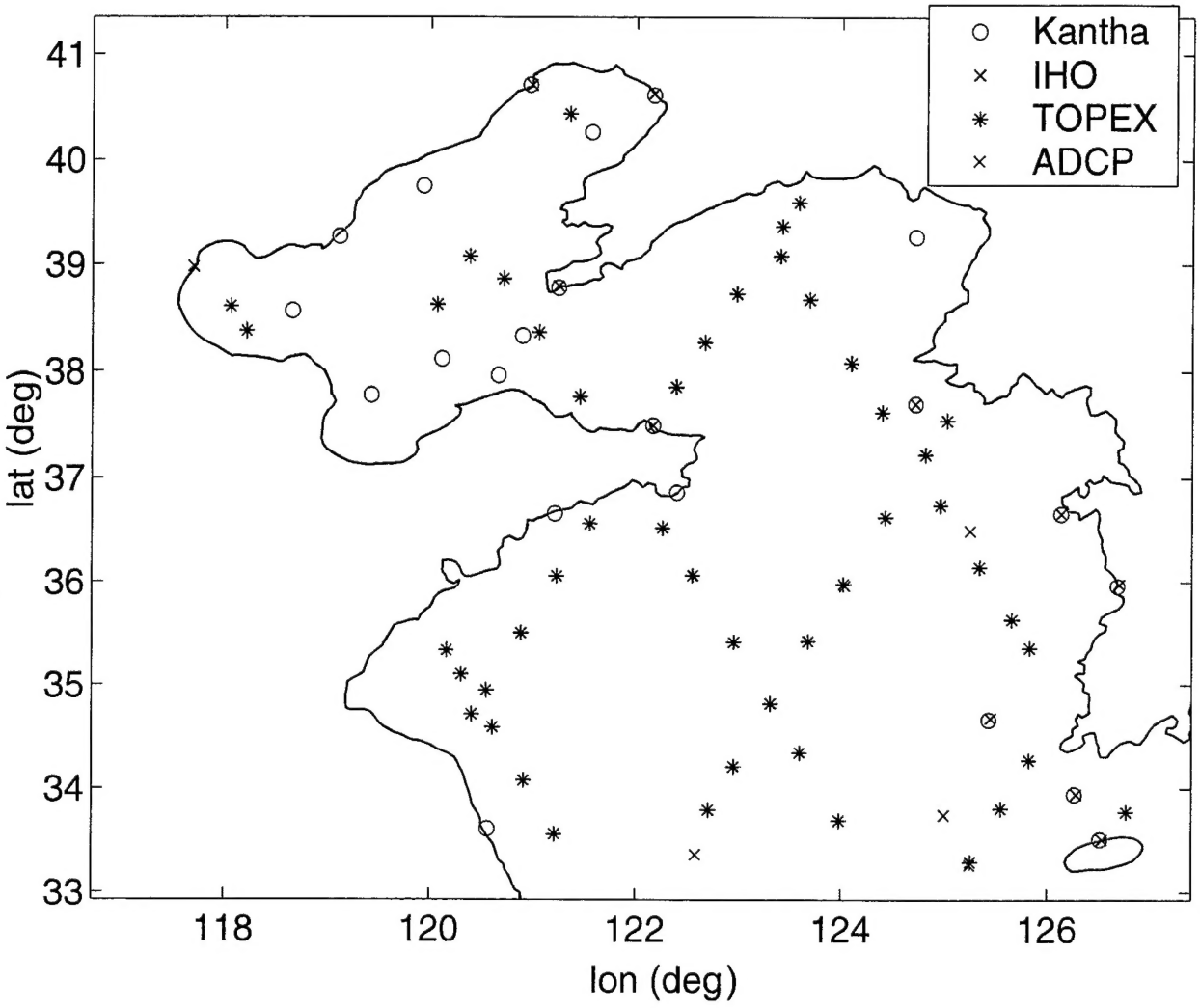

Fig. 2 — A map of elevation stations and ADCP locations used for assimilation and comparison to model results

generalized least-squares regression (Griffin and Thompson 1996; Pistek et al. 1998; Thompson and Griffin 1998).

3. APPLICATION TO THE YELLOW SEA

The incremental approach is applied here to tidal dynamics in the Yellow Sea, the semi-enclosed sea between China's east coast and Korea (Fig. 3). This marginal sea is one of the largest shallow areas of continental shelf in the world. In addition, there exist sufficient observed data to effectively use adjoint methods in the region.

The coastline of the region is quite complex, which requires increasing resolution nearshore for proper coastal representation. For this reason, applications of a complex model over limited domains using open boundary information obtained from the incremental approach applied over a larger grid are explored. Given proper information at the open boundary of the limited area domain, the use of limited area domain models can allow even greater refinement nearshore without sacrificing computational time.

3.1 Station Data

Tidal elevations are obtained from the International Hydrographic Office (IHO) tidal stations, select points along TOPEX-POSEIDON altimeter tracks, station data from L. Kantha (University of Colorado), and three ADCP records collected by the U.S. Naval Oceanographic Office. Figure 2 is a map showing the geographical locations and source of data. Data at IHO stations located beyond the boundaries of the finite difference grid used by the linear ADJOINT model, for example, up rivers or inside harbors, are discarded from the dataset and are not shown in Fig. 2.

All comparisons are made for the month of September 1995, an interval when winds were weak and the observations are dominated by tides (Perkins and Pistek 1998). Time series from all stations were vertically integrated to make them compatible with the assimilation dynamics, then detided and reconstructed to a month-long, half-hour dataset comprising the four main tidal constituents (O_1, K_1, M_2, and S_2). This later time series forms the basis for comparison with model solutions.

3.2 Grids

Current NAVOCEANO tidal predictions in the Yellow Sea are obtained from a tidal database created by the Army Corps of Engineers. The database is derived from an ADCIRC model solution computed on a finite element grid that is known to under-resolve the speed of a gravity wave using a dimensionless wavelength criterion (LeProvost and Vincent 1986; Westerink et al. 1994b,c). This *fareast* grid (Fig. 4), with its open boundary well off the continental shelf into the Pacific Ocean, was a first attempt at creating a finite element grid for applications in the Yellow Sea and Sea of Japan with finite element hydrodynamic models such as ADCIRC, FUNDY, and QUODDY.

The ADCIRC solution over the *fareast* grid shows mediocre agreement with station data (Fig. 5). The solution at TOPEX stations in the interior of the domain exhibits poor agreement with data (i.e., errors between 10 and 30 cm). Areas where the largest disagreement with data can be found are located off the Chinese coast near the entrance to the Yellow Sea and at tidal stations near the Kyunggi and Seahan Bays off the Korean coast, where errors exceed 60 cm in root mean square (RMS) error. This deterioration of the solution along the path of the Kelvin

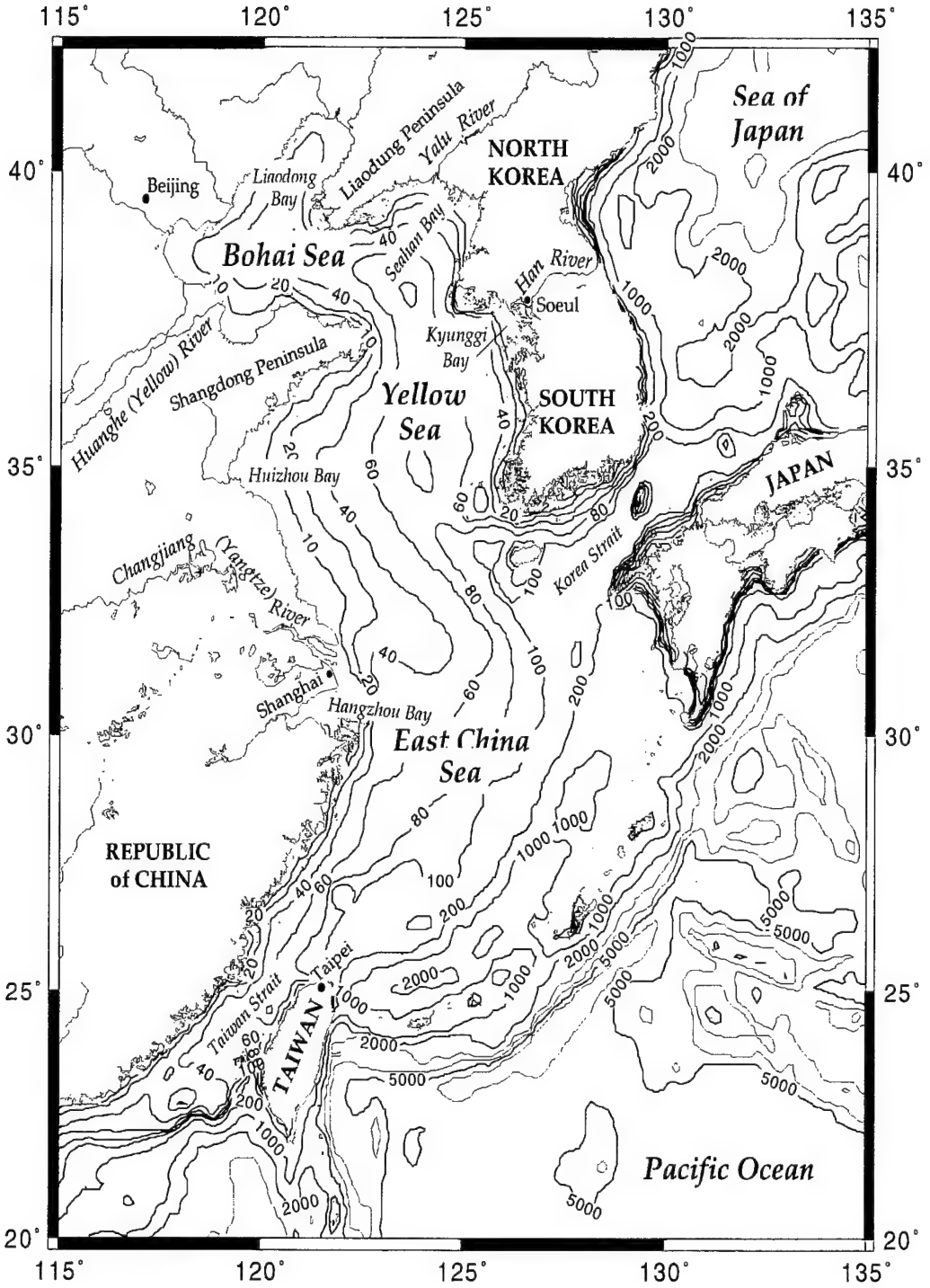

Fig. 3 — Bathymetry in the Yellow Sea. Depth is shown in meters.

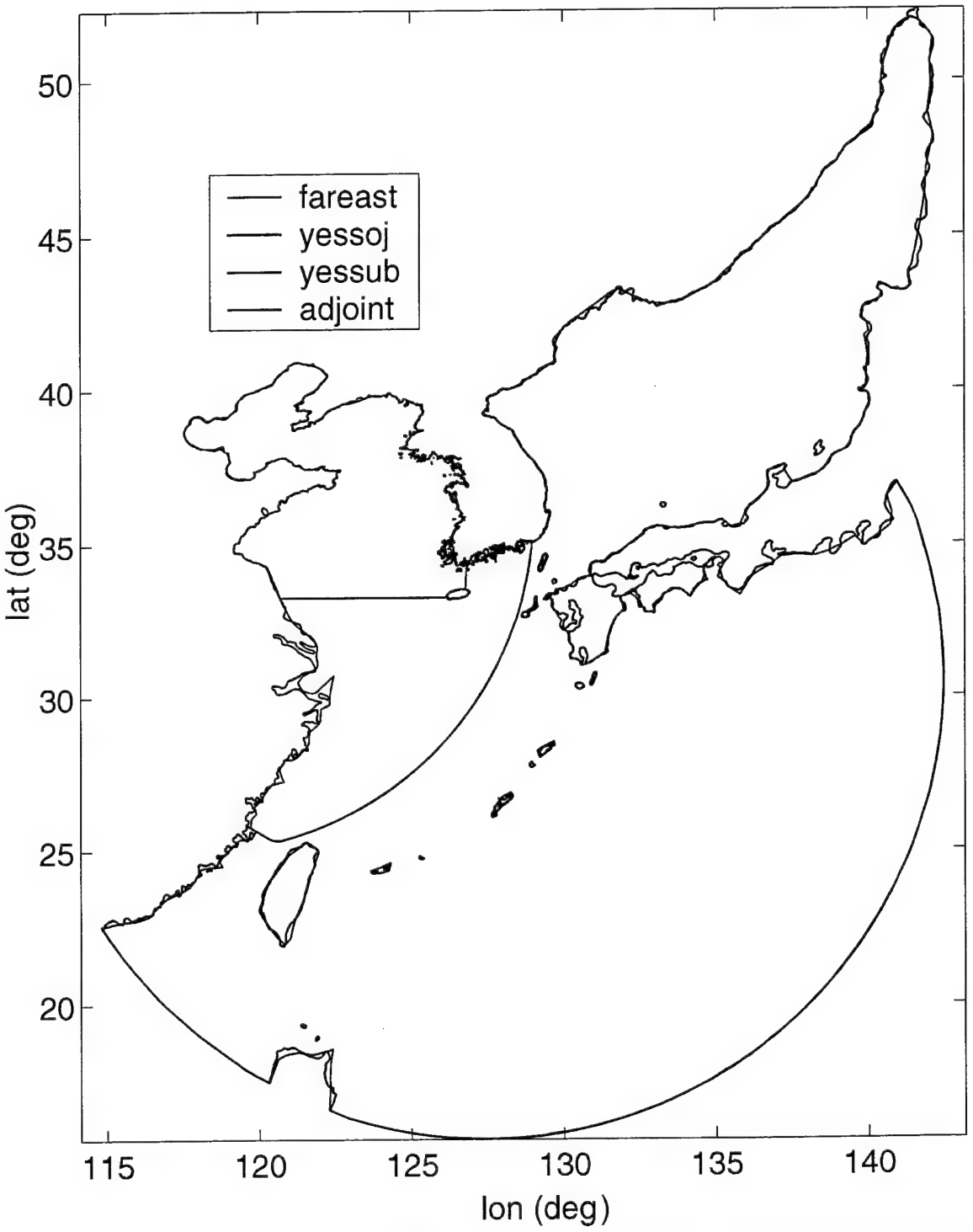

Fig. 4 — The *yessoj* family of grids, shown with the original *fareast* grid. The only variation from the largest grid is the placement of the open boundary.

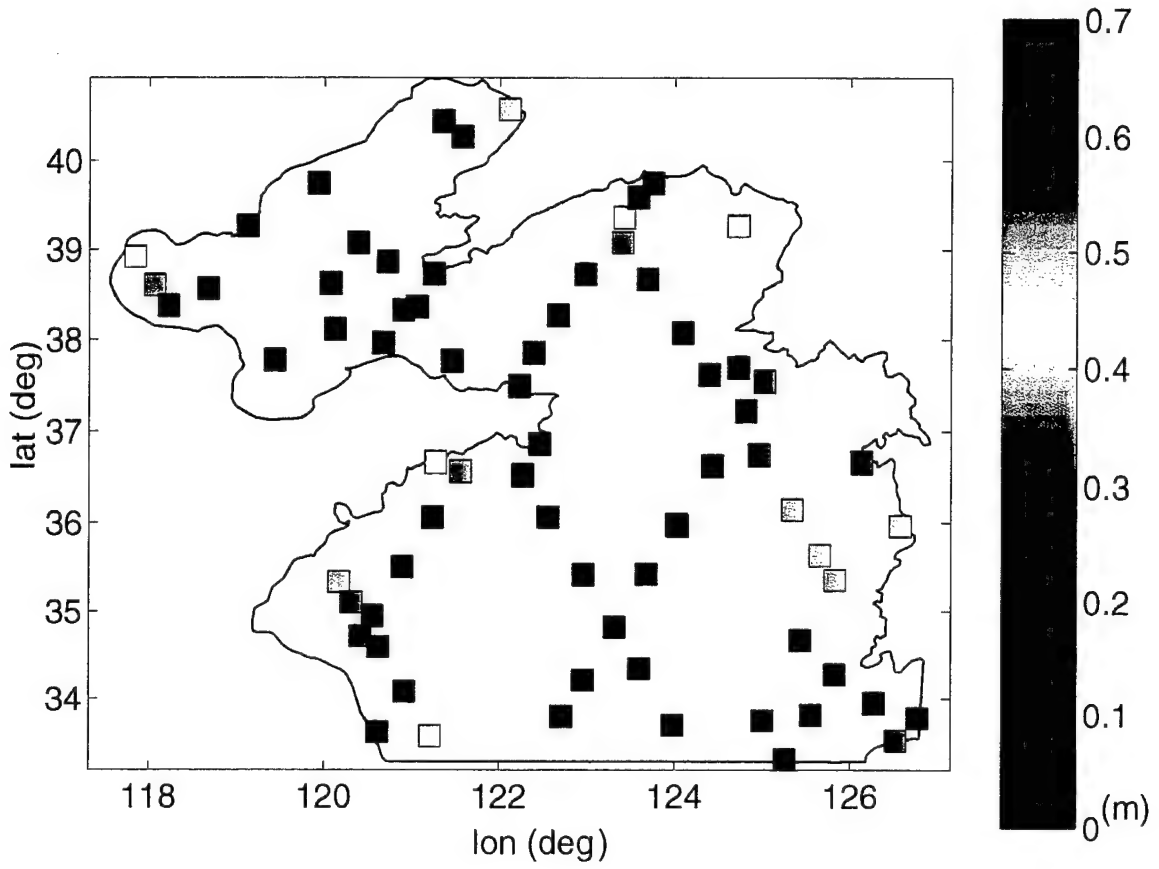

Fig. 5 — Time series tidal elevation error by station for the *fareast* grid. RMS error in meters.

wave (Jacobs et al. 1998) from the southeast into the interior and its exit from the basin in the southwest indicates a problem with the grid itself rather than with the solution method.

As a packet of waves travels into progressively shallower water, its group velocity decreases, and greater resolution is necessary to resolve the waves. The *fareast* grid is inherently destructive in that it does not properly resolve the M_2 tidal signal as it propagates across the shelf and into nearshore regions within the domain (Fig. 5). To correct this deficiency, a new family of grids for the Yellow Sea-Sea of Japan is created to replace the *fareast* grid.

The *yessoj* grid (Fig. 4), like the *fareast* grid, extends radially outward from the Yellow Sea, encompassing the East China, Philippine, and Japan Seas and extending into the deep water of the Pacific Ocean. The open boundary stretches from just north of Hong Kong, through the Philippine Sea and deep waters of the Pacific Ocean, to just north of Tokyo, Japan (see Fig. 3). Bathymetry ranges from an imposed minimum of 2 m in the shallowest waters of the Bohai Sea to over 8000 m in the Western Pacific Ocean at the easternmost section of the grid. The resolution in nearshore regions, especially in the Bohai Sea, is fine tuned (Fig. 6) to resolve a range of tidal frequencies, increasing nearshore resolution to unmask smaller scale features within the flow.

Resolution increases dramatically at the shelf break, around islands in the southwestern part of the domain, and around Japan. On the shelf of the Yellow Sea, resolution of the *yessoj* grid (Fig. 6a) increases in the Bohai Sea and very close to land, but decreases slightly in the center of the Yellow Sea, where gravity wave speed permits slightly lower resolution than that specified by the *fareast* grid (Fig. 6b).

The bathymetric depths for the Bohai, Yellow, and East China Seas (depths less than 200 m) are determined from a high resolution data set distributed by C. Horton at NAVOCEANO in 1995 (Fig. 3). These data originated from South Korean sources and were compiled and processed by L. H. Kantha at the University of Colorado. The spatial resolution for this data is 5 minutes in longitude and 4 minutes in latitude. For locations where depths exceed 200 m, bathymetry is derived from the NAVOCEANO Digital Bathymetric Data Base - 5 minute resolution (DBDB-5). Additionally, an updated bathymetry was included in the Yellow Sea north of the 34° N line of latitude. Adjustments to the bathymetry are made based on preliminary ADJOINT experiments. These modifications are included for compatibility between the forward and adjoint model bathymetry.

From the *yessoj* grid, a family of grids (Fig. 4) is created with open boundaries positioned successively farther into the Yellow Sea on the continental shelf. All domains used here extend outward from the Bohai Sea and cover areas of decreasing size. By retaining the same resolution throughout the domain and changing only the placement of the open boundary, the effect of large vs limited area domains can be investigated in conjunction with ADJOINT model experiments.

4. MODEL EXPERIMENTS

4.1 Non-assimilative Experiments

The initial *yessoj* solution is forced by tidal potential forcing and specified elevations on the open boundary derived from eight tidal frequencies taken from the Grenoble global tidal database (Le Provost et al. 1994). Though the results were analyzed with respect to only four primary constituents, the M_2, S_2, O_1 and K_1, the K_2, N_2, P_1, and Q_1 tidal frequencies are included in open boundary forcing for completeness.

Figure 7 shows the cotidal chart for M_2 dynamics. Two amphidromes are located off the Chinese coast, and another just offshore from the entrance into the Bohai Sea. M_2 elevation increases as the tidal wave propagates onto the shelf, up the Korean coast, and into Kyunggi Bay near Seoul (Fig. 3). Amplification of the M_2 tide is also pronounced in the Tsushima Strait separating Taiwan and mainland China. Current residuals through the domain are generally small (3 to 6 cm/s), except near islands in the East China and Japan Seas, where they range from 10 to 25 cm/s in magnitude. These larger residual currents may be an indication of under-resolution of the mesh in these regions of steep topographic gradients.

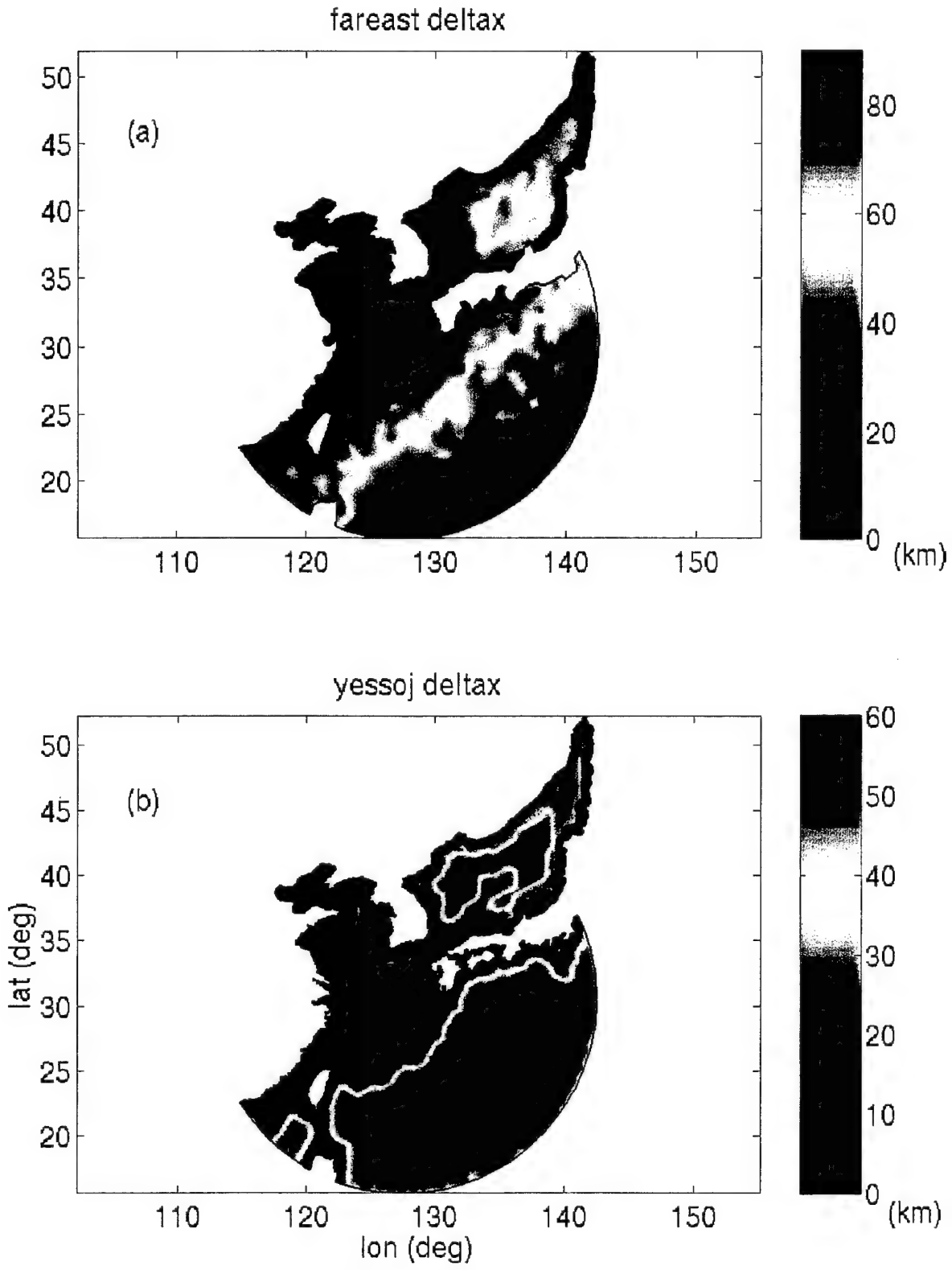

Fig. 6 — Grid resolution for (a) *fareast* and (b) *yessoj* grids

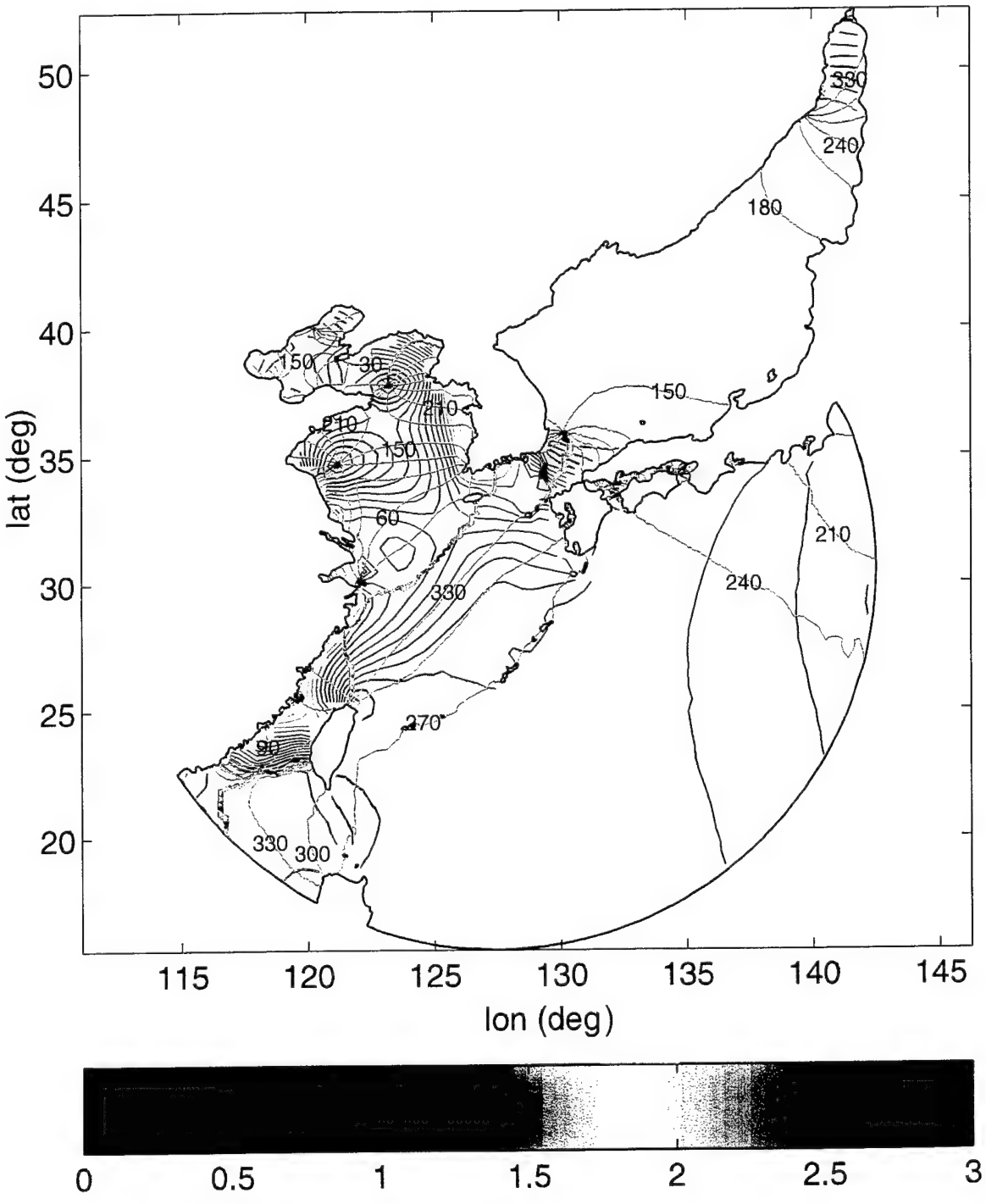

Fig. 7 — Co-range lines are shown in color, with magnitude in meters corresponding to the colorbar above. Co-phase lines (in degrees) are plotted in increments of 30 degrees, and are shown in brown.

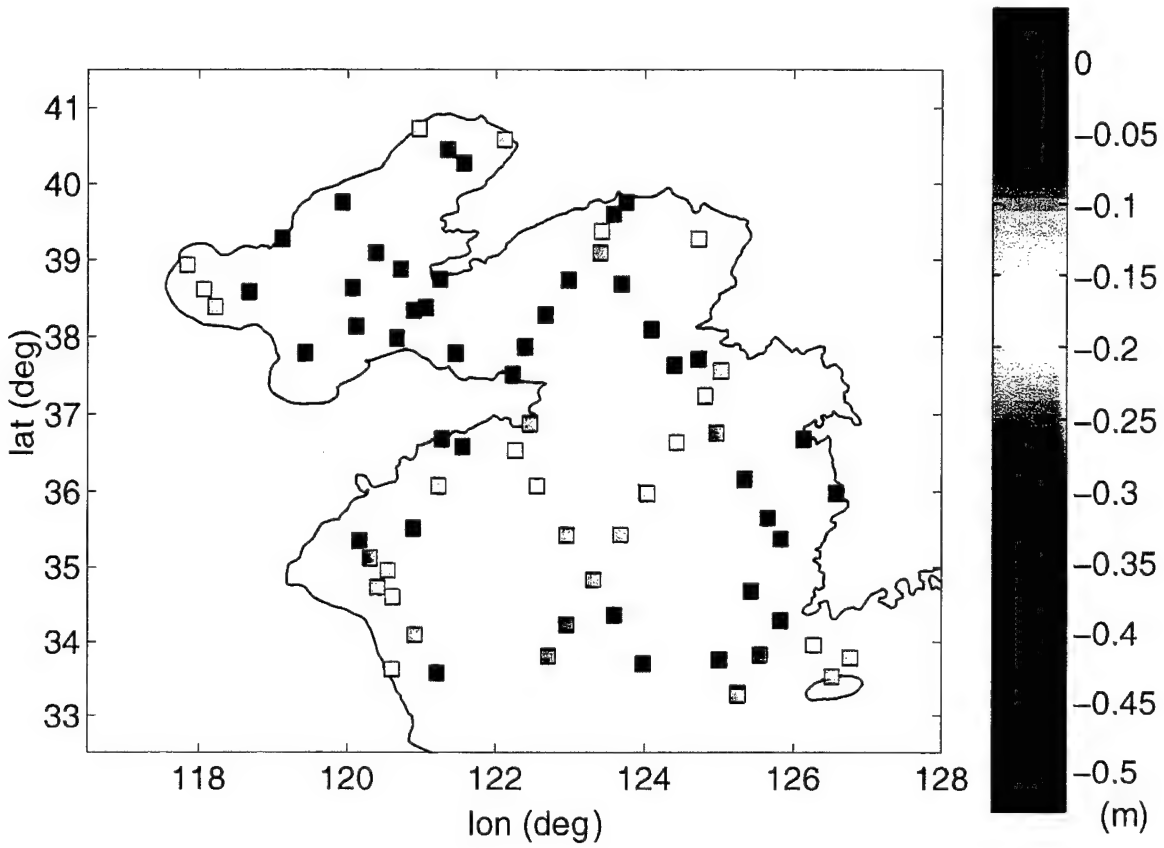

Fig. 8 — Difference (*yessoj-fareast*) in mean absolute error by station. Magnitude of the difference is color-coded in meters.

Comparison with the observational station data shows significant improvement of mean absolute error over the *fareast* solution at all 80 stations analyzed (Fig. 8), ranging from a 5 cm improvement through the interior of the domain to as much as 50 cm at the tidal stations near the coast. The greatest improvement was seen at the tidal stations nearest the coastlines in shallow water, where the solution improved on the order of 50% to 80%, from 70 cm to 20 cm in mean absolute error.

The finite element grid *adjoint* (Fig. 4) is created to match exactly the boundaries of the finite difference grid used with the linear ADJOINT model. The initial open boundary of this grid stretches from the coast of China at Yancheng, well inside the shelf-break, at approximately 33.25° N latitude. Interpolation from the global tidal database used previously (Grenoble) is clearly inappropriate for a boundary located this far onto the continental shelf. Thus, the *yessoj* solution is interpolated to the *adjoint* open boundary nodes and used as elevation forcing on the boundary.

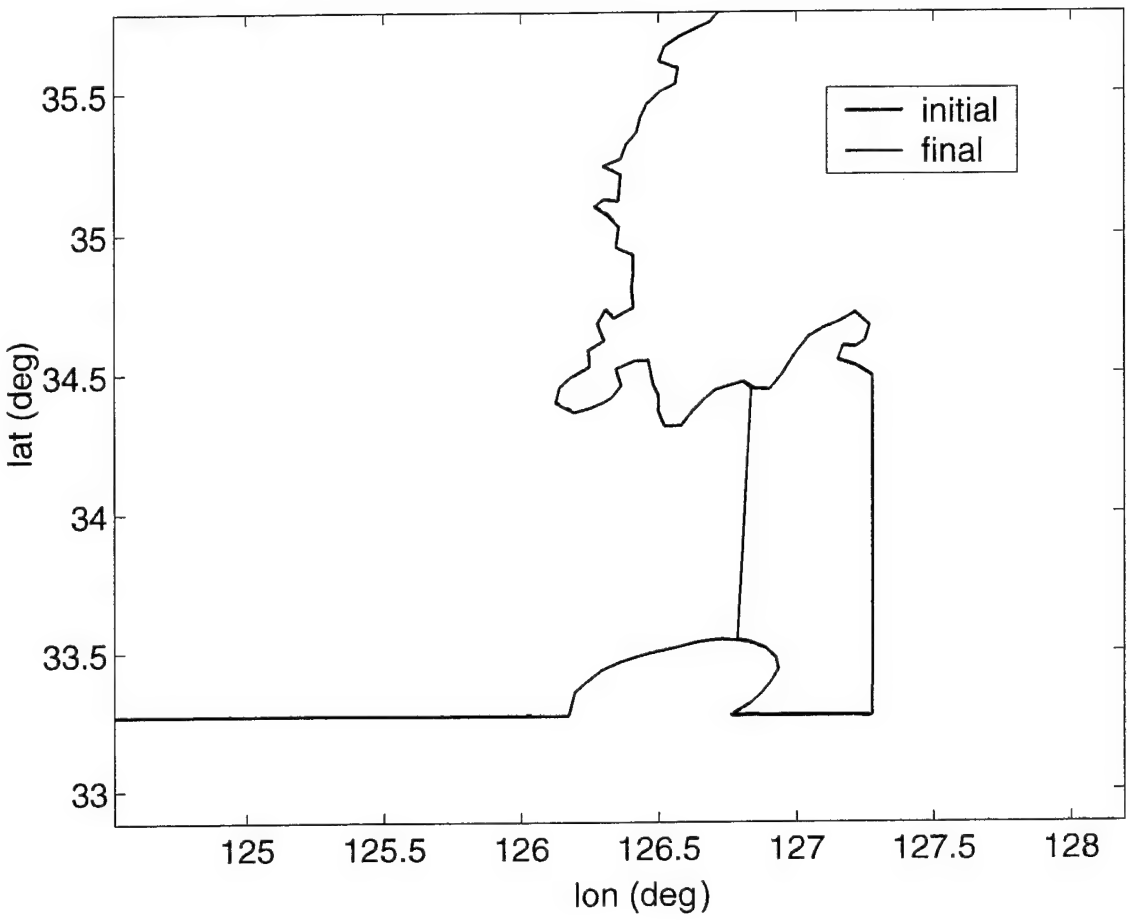

Fig. 9 — The open boundaries of the initial (blue) and final (black) versions of the *adjoint* grid

The combination of the boundary placement through Cheju Island, and a 90° corner in the open boundary of the new grid proved problematic (blue line in Fig. 9). Circulation around Cheju Island which had developed in the *yessoj* solution now used as forcing is constrained by the essential elevation boundary condition as applied in the *adjoint* model. A nonphysical compensating flow in the tidal residual currents emerges, and exhibits signs of numerical instability because of the sharp corner and ill-posed boundary specifications.

A series of experiments having varied specification of a radiation boundary condition along the open ocean boundaries of the *adjoint* grid aim to recapture a dynamically consistent residual flow near Cheju Island. Instead of specifying elevation on the open boundary, the boundary is treated as a natural boundary allowing wave radiation normal to the boundary (Luettich et al. 1992; Westerink et al. 1994a). This radiation condition is applied by specifying the contribution to the normal boundary flux integral in the continuity equation, a formulation that is unique to

the finite element Generalized Wave Continuity Equation-based models (Luettich et al. 1992; Kolar et al. 1994a,b; Westerink et al. 1994b). In this formulation, there is no constraint on velocity (normal or tangential) in the momentum equations; thus, waves are allowed to propagate freely out of the domain. The flow normal to the boundary is computed using a Sommerfeld radiation condition (Roed and Smedstad 1984). This boundary condition correctly satisfies the flux balance in a global sense, but only satisfies the normal flow at each boundary node in the limit of infinite resolution (Westerink et al. 1994b).

The flux specified as part of the radiation boundary condition implementation is interpolated from the *yessoj* solution in the same manner as for specified elevations. Four radiation boundary regimes are considered: a) contiguous implementation on the open boundaries north and east of Cheju island, b) implementation separately along the north and east segments of these open boundaries, c) implementation of the radiation boundary condition on the north segment and specifying elevation on the east segment (and vice versa), and d) implementation of a contiguous radiation boundary condition as in a), but now "tacking down" the solution at the juncture of the north and east boundary segments with five specified elevation boundary nodes. Despite these various configurations of the radiation boundary conditions, the 90° corner in the grid remained problematic in its generation of a numerically spurious solution. As a final solution, the grid was modified, moving the eastern boundary westward such that the boundary now extends from the Korean coast directly south to Cheju Island (black line in Fig. 9).

As mentioned previously, bottom topography in the Yellow Sea ranges from mud flats in the Bohai Sea to rocky, jagged terrain off the South Korean coast. Recall that the linear ADJOINT model uses spatially varying coefficients for the linear friction formulation over the domain (Fig. 1). Dimensionless values range from 0.01 in the Liaodong Bay in the northeastern Bohai Sea to 0.18 off the South Korean coast in the east. To investigate the possibility of including spatially variable friction coefficients for use with the quadratic bottom stress formulation in ADCIRC, a series of model runs are conducted with a spatially constant friction coefficient, C_f, set to 0.0015, 0.002, and 0.0025. The results from these three runs are compared to station data.

RMS error is calculated by station, and analyzed with respect to station type and geographical location. In general, it is found that data at most stations agree best with model results using frictional values of $C_f = 0.002$ and 0.0025. The exception is in the middle of the basin (Fig. 10), where the friction coefficient of 0.0015 resulted in smaller RMS errors. It is interesting to note that the observations at stations in the Bohai Sea agree best with the friction values of 0.002 and 0.0025. Minimum errors at TOPEX track stations are recorded using the lowest friction coefficient, $C_f = 0.0015$.

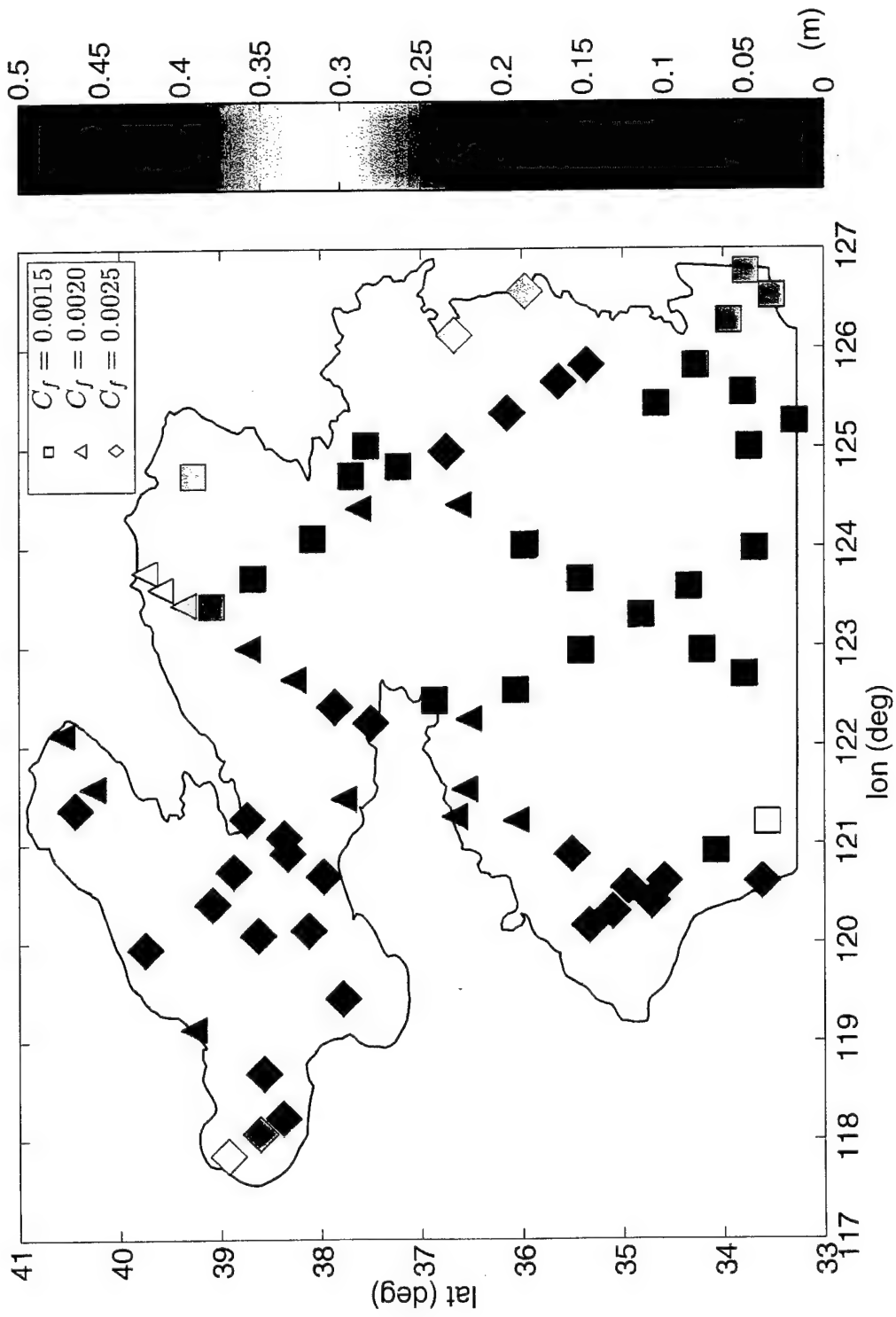

Fig. 10 — Minimum error by station for varying C_f. Color of the error shape represents the magnitude of the minimum root mean square error in meters. Shape represents which frictional value produced that minimum.

From this set of experiments, it becomes clear that specifying complicated spatially variable drag coefficients over the majority of the domain provides relatively little improvement. The nearshore regions off the Korean coast post the largest RMS errors yet appear relatively insensitive to the frictional coefficient. For all remaining ADCIRC model simulations, a constant frictional coefficient of 0.0025 is used.

4.2 Assimilative Experiments

With the open boundary of the *adjoint* grid coincident with the open boundary of the finite difference ADJOINT model, the complex forward model ADCIRC is forced using open boundary values generated by the solution of the simple linear ADJOINT model. Model-data misfits between the forward model predictions and observed elevation and velocity time series at data stations are assimilated by the ADJOINT model. Optimal boundary conditions are then derived by minimizing this error between the forward model and the data.

Flux from the ADJOINT model solution is interpolated to the open boundary of the *adjoint* grid for each of the four constituents previously analyzed, the M_2, S_2, O_1, and K_1. The difference in resolution along the boundary of the two grids (40 km vs 4-20 km) results in discrepancies in the land/sea interface. As such, it is necessary to extrapolate the fluxes at the eastern and westernmost open boundary nodes of the ADJOINT model to the *adjoint* grid nodes that extend to the mainland using a band-limited reconstruction technique. In this approach, the magnitude of the flux is tapered sinusoidally towards a mean flux (computed from the linear ADJOINT model solution) at the mainland. Despite the large differences in resolution, flux from the linear ADJOINT model solution is sufficiently smooth for interpolation to interior grid points along the *adjoint* finite element grid open boundary.

Cast as the complex forward model in iteration with the simple ADJOINT model, ADCIRC is then run, forced by this specified normal flux on the open boundary. Within ADCIRC, the normal flux is represented by essential boundary condition with no constraint on tangential flow at the open boundary nodes. This boundary condition implemention requires specifying a nonzero contribution to the normal boundary flux integral in the continuity equation and a nonzero normal velocity in the momentum equations. A flux balance is achieved in a global sense between the two models while satisfying the need for a normal flux at each boundary node. Upon completion of an ADCIRC model simulation on the *adjoint* grid, a time series at each station is created from the ADCIRC elevation and velocity solutions. The linear ADJOINT model is then run with these time series representing deviations from the observational data used previously. This latter ADJOINT model solution at the open boundary is then reinterpolated and extrapolated to the complex model *adjoint* grid boundary and the iteration begins again.

In this application to the Yellow Sea, each successive iteration yields model-data misfits between the forward model and the observations that grow in magnitude, indicating divergence

of the solutions. To test the role of the band-limited extrapolation scheme in this divergence, boundary values at grid nodes in the extrapolation region are assigned velocities interpolated from the *yessoj* solution (Fig. 11). This scheme improves the forward model solution slightly with respect to RMS errors, but when further iterated with the ADJOINT model, the solutions continue to diverge.

Given the experiences thus far and knowing that the incremental data assimilative approach is limited by the proximity of the simple model dynamics to the Jacobian of the complex model, a simple twin experiment is designed to determine whether convergence of this forward-inverse model system is possible. An ADCIRC solution is obtained for a simple M_2 flux forcing across the open boundary. Assuming that the ADCIRC model predictions exactly match the observations at the 80 locations previously identified, the ADJOINT model should recover the M_2 flux forcing along its open boundary. However, the linear ADJOINT model is unable to recover this simple forcing at its open boundary with the ADCIRC computed elevation and velocity time series assimilated at 80 observation points (personal communication, J. Book).

This result suggests that convergence between the two models in this application is unlikely and may be the result of known incompatibilities between the models. It is well known that a properly formulated ADJOINT model is derived from the linearized discrete form of the forward model (Bennett, 1992; Thompson *et al.*, 2000). This ensures that the minimization search proceeds in a direction appropriate for determination of the true minimum. ADCIRC-2DDI is based on a Generalized Wave Continuity Equation-based formulation of the shallow water equations and discretized using finite element methods (Luettich et al., 1992; Kolar et al., 1994a,b; Westerink et al., 1994a). In contrast, the ADJOINT model is a finite difference discretization of the linearized primitive shallow water equations. While the forward and inverse adjoint models of the linear system are well-posed, the inverse of the ADJOINT model is not a proper adjoint formulation for the complex forward model. Though this incompatibility was known at the onset of this application to the Yellow Sea, the question remained whether this incompatibility precludes improvements to the forward model solution from such an implementation of the incremental approach. An answer to this question is still unknown as there are several other model incompatibilities that may be affecting the success of the methodology.

Several differences between the models complicate the issue of convergence using the incremental approach. Namely, the resolutions and computational grids of the complex forward model and the simple ADJOINT model are disparate. Computations for the ADCIRC model are obtained over a highly resolved triangular mesh (resolution ranges from 4 to 20 km along the open ocean boundary). The ADJOINT model solution is relative to an Arakawa C-grid having 40 km resolution, almost 1/10th the resolution of the complex forward model grid.

It should be noted that for the strong constraint inverse problem, the linear ADJOINT model exactly matches linear dynamics in the interior of the domain. At the open boundary, an optimal

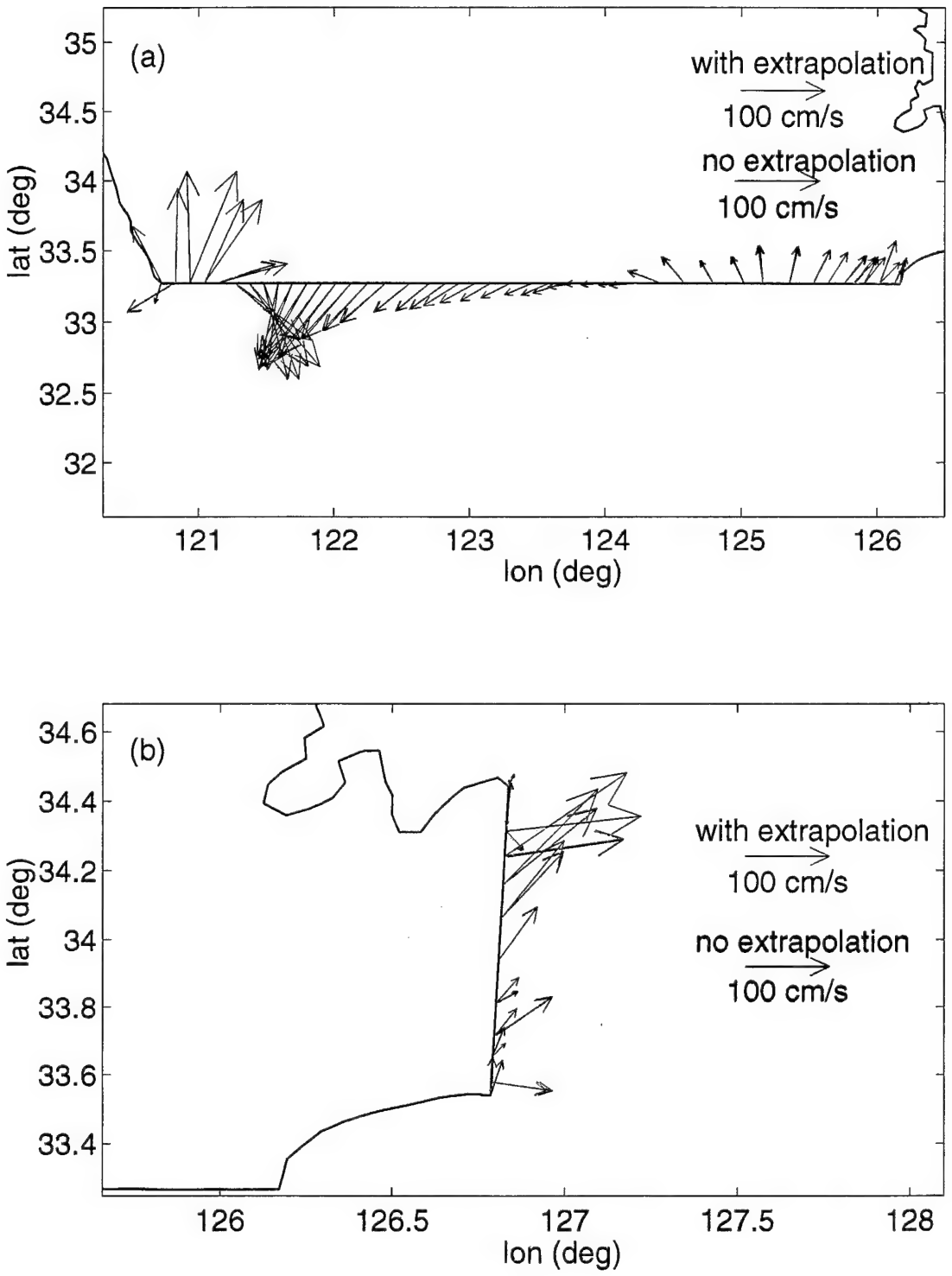

Fig. 11 — M_2 velocity corresponding the specified flux applied at the southern (a) and eastern (b) open boundaries of the *adjoint* grid. The extrapolation/interpolation scheme is shown in red, and *yessoj* solution substitution/interpolation in blue.

solution is derived subject to the dynamical equations and a minimization of the forward model-data misfit. Comparing the original *yessoj* solution at the *adjoint* grid boundary locations to the fluxes generated by the solution of the linear ADJOINT model system illustrates the difference between the optimal and purely dynamical model boundary forcings (Fig. 12). "Iteration 1" velocities in Fig. 12 represent boundary forcings derived from the linear ADJOINT model given model-data misfits obtained using ADCIRC elevations and velocities (as computed using the open boundary forcing shown in red). Large gradients in normal flux forcing are evident, even as much as a 180 degree phase change over less than 100 km in the westernmost section of the open boundary, and the magnitude of this gradient grows substantially between iterations of the linear ADJOINT model system. It is likely that the coarse resolution of the ADJOINT model is a primary cause and the conflicting land/sea boundary locations are a secondary cause of the boundary value discrepancies depicted in Fig. 12. The effect is divergence of the incremental approach applied to the ADCIRC and ADJOINT models as configured.

Lastly, the differences in the implementation of the boundary conditions may also contribute to the divergence of the incremental approach as applied here. When forcing with specified elevation or flux as an essential boundary condition, ADCIRC regards such information at the open boundary nodes as known. Thus, in the Generalized Wave Continuity Equation solution matrix, the equations associated with those boundary nodes are eliminated. In contrast, the open boundary condition of the linear ADJOINT model radiates about both elevation and velocity at the open boundary as calculated by the inverse model, using the boundary condition (9) to minimize reflection. This mismatch in boundary condition formulation between the complex forward model and the linear ADJOINT model likely contributes to increasing the distance between the Jacobian of the complex model and that of the simple ADJOINT model. According to Thompson et al. (1998), this effect can be destructive to the convergence of the solution using the incremental approach.

In summary, several factors limit the success of the data assimilative incremental approach as applied here. These include incompatibility of the complex forward model and the simple ADJOINT model, disparity in resolution of the grids used by the complex and simple forward models, and different boundary condition implementations. The extent to which each of these factors influences convergence of the incremental approach is yet to be determined. Certainly, this work demonstrates the need to consider these issues of compatibility when implementing a data assimilative approach.

4.3 Limited Area Domains

One alternative to the incremental approach that includes a complex forward model explicitly within the assimilation loop is to simply interpolate the optimal solution obtained from the linear forward/inverse ADJOINT model system to the open boundary of the complex forward model

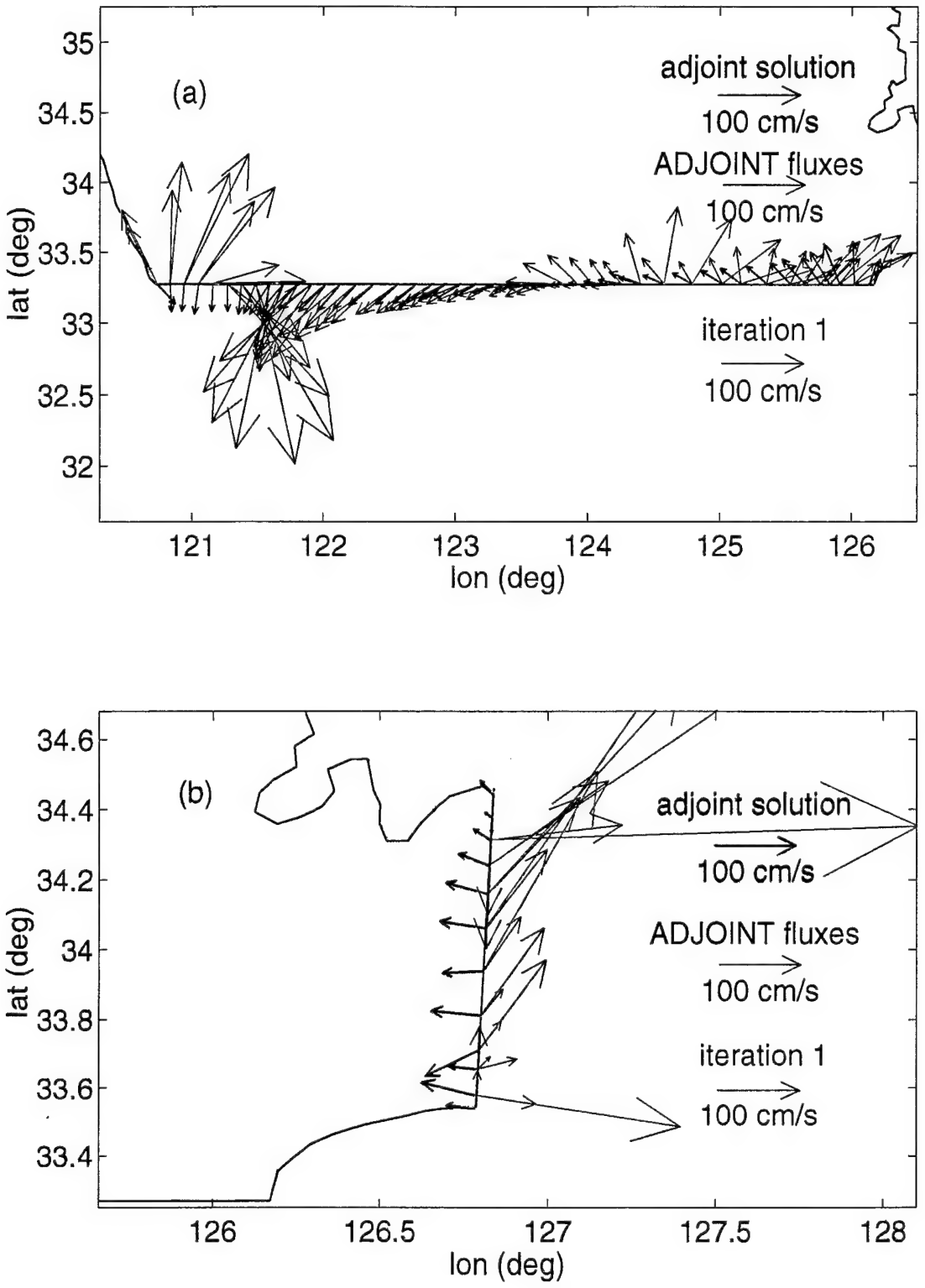

Fig. 12 — M_2 velocities on the southern (a) and eastern (b) open boundaries are shown for the *adjoint* solution computed with *yessoj* forcings (blue), forcings interpolated from the linear ADJOINT model solution (red), and the ADCIRC solution "iteration 1" (cyan).

applied over a limited domain. In this instance, limited domain implies that the nonlinear forward model open ocean boundary is contained within the linear ADJOINT model domain.

In order to test this approach for obtaining boundary forcings for the nonlinear model, a family of limited area domains is created from the original *yessoj* grid, with the open boundaries positioned successively further into the Yellow Sea on the continental shelf (Fig. 13). Tidal elevations are interpolated from the linear ADJOINT solution to the open boundaries of the limited area grids for each of the four constituents previously analyzed. The complex model, ADCIRC, is then executed over each of these grids using this interpolated forcing. The results are then compared to the linear ADJOINT model solutions that include data assimilation.

yesbit

Figure 14 shows the difference in mean absolute error between the ADCIRC solution of the *yesbit* grid, produced with forcing interpolated from the original *yessoj* solution, and the ADCIRC solution forced by the interpolated linear ADJOINT model solution (denoted "yesbit i1"). Positive values indicate that greater errors occur in the nonassimilative *yesbit* solution. Differences are small in the interior of the basin and, surprisingly, in the Bohai Sea, but increase in magnitude along the eastern and western shores of the Yellow Sea, with greatest differences at tidal stations just off the coast.

subadj

The open boundary of the *subadj* grid is selected as a straight line between an altimeter station and a Kantha elevation station. Solutions over this finite element grid are forced in a similar manner as for the *yesbit* experiment. Elevations at open boundary nodes are derived by interpolation from the interior solution of the linear ADJOINT model. Figure 15 shows the difference in error between the solutions. Again, positive differences represent greater error in the *subadj* solution forced by *yessoj* elevations. Differences in error between the solutions, for the most part, are quite small (<1.0 cm RMS). However, for this grid, the original *subadj* solution outperforms the data assimilative ("i1") solution that uses 46 of the 58 total stations that lie in the *subadj* domain giving smaller RMS errors (elevation). The exceptions are at two stations that lie along the open boundary, where errors of 20 cm are recorded.

subadj2

A third limited area domain is defined (*subadj2*), with its open boundary located even further into the interior of the Yellow Sea. Solutions are computed in an analogous manner as previous limited area domains, and the errors are analyzed for both simulations. Fig. refsub2 shows a comparison of RMS errors of the results.

As with the comparisons for the *subadj* grid solutions, use of the assimilative open boundary forcing improves the solution significantly on the open boundary. However, unlike the *subadj*

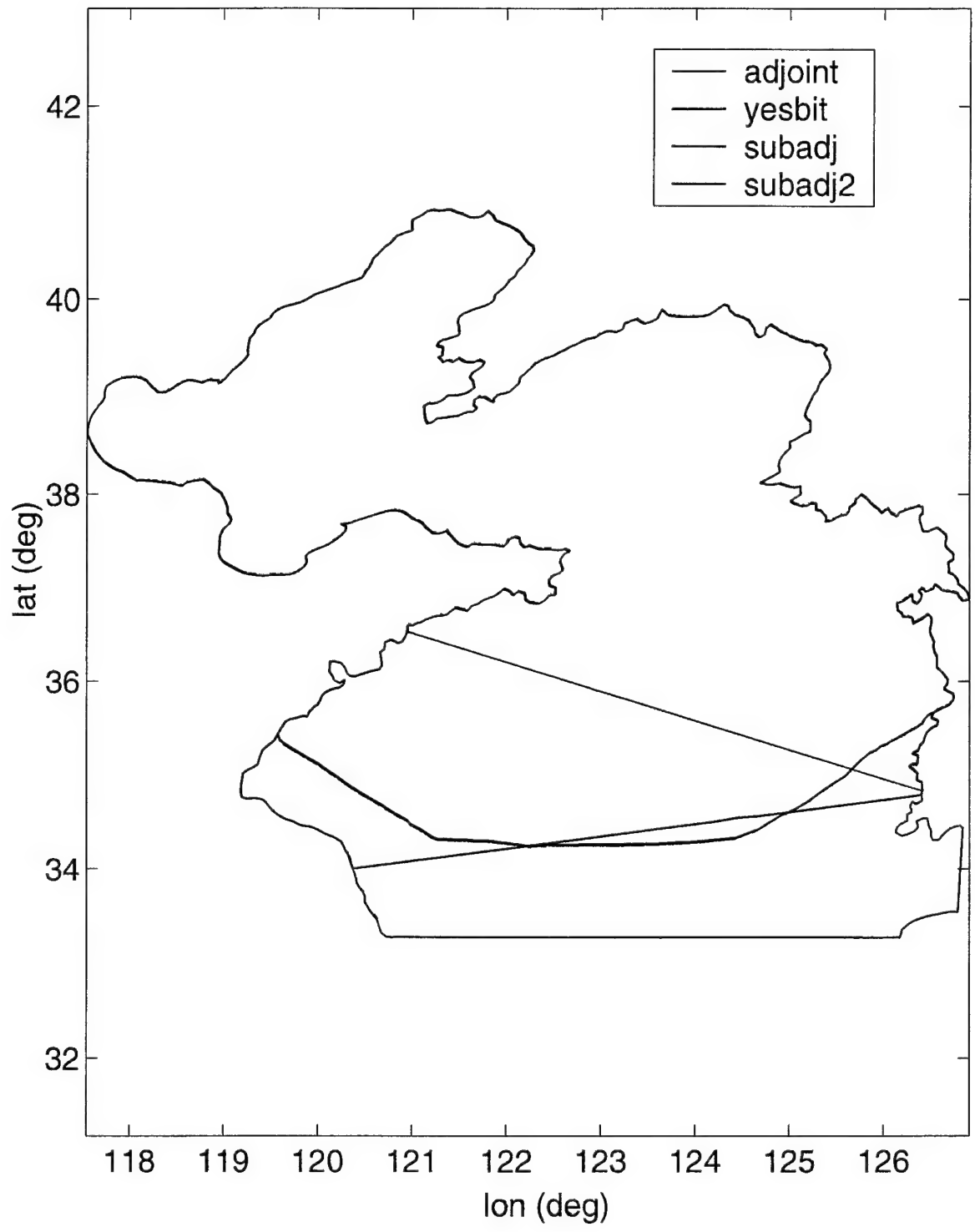

Fig. 13 — Limited area domain grids, plotted with the *adjoint* grid used in previous ADJOINT experiments

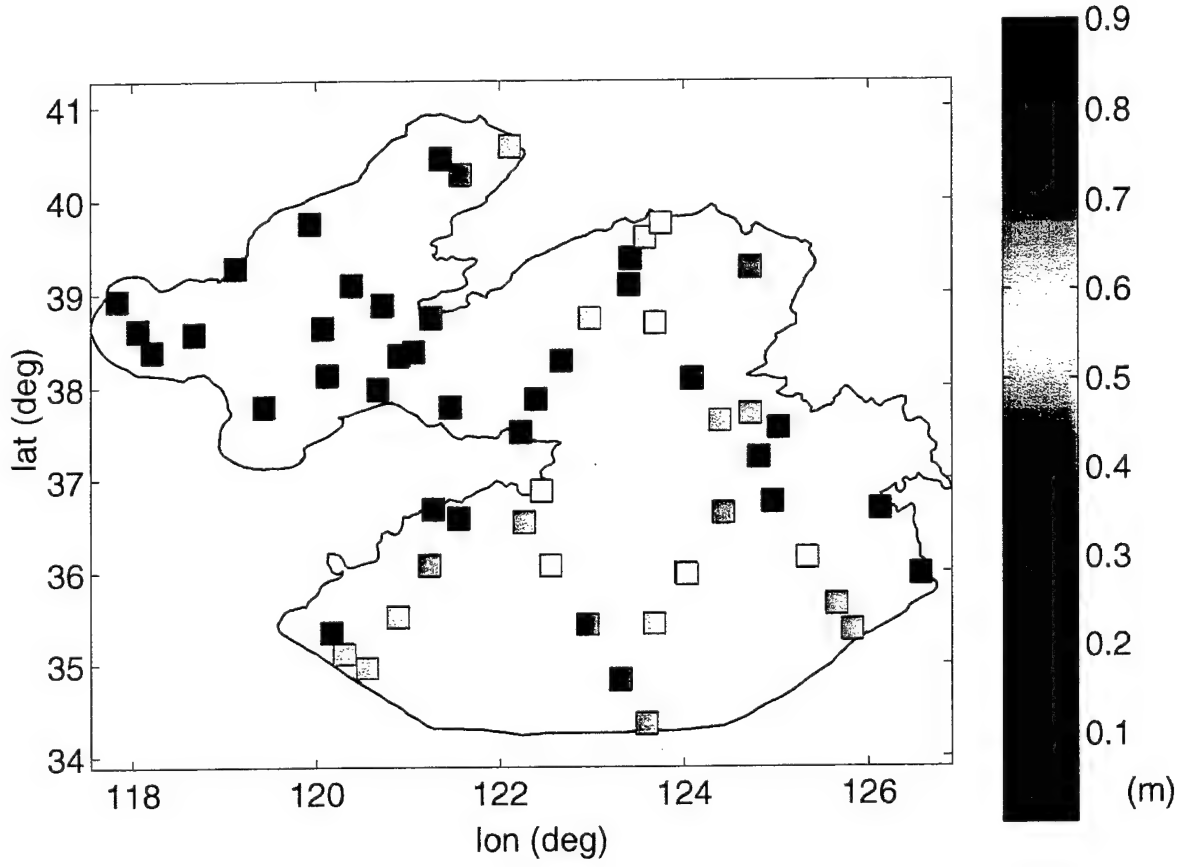

Fig. 14 — Mean absolute error by station for the difference between the *yesbit* solution (forced by the *yessoj* solution) and the "yesbit i1" solution produced with forcing interpolated from the linear ADJOINT model

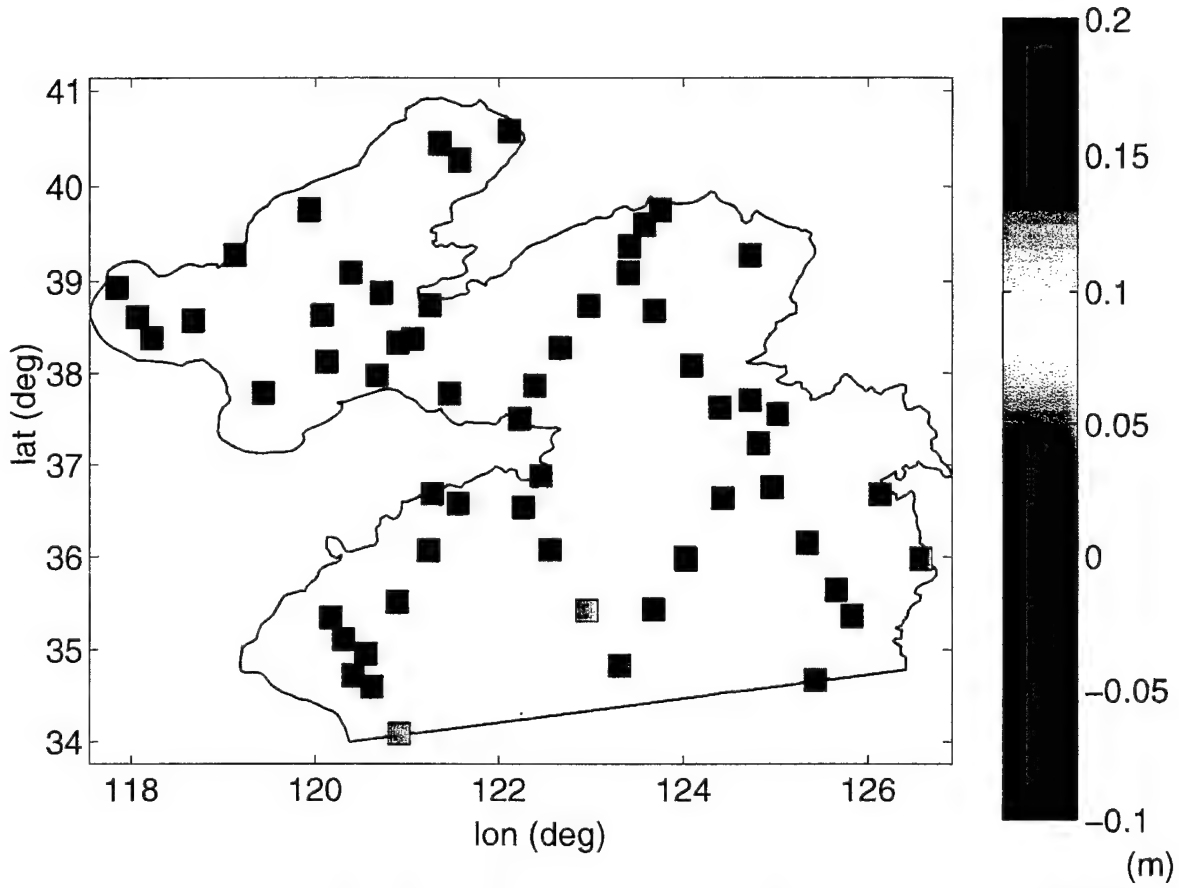

Fig. 15 — Root mean error by station for the difference between the *subadj* solution and the "subadj i1" solution produced with forcing interpolated from the linear ADJOINT model

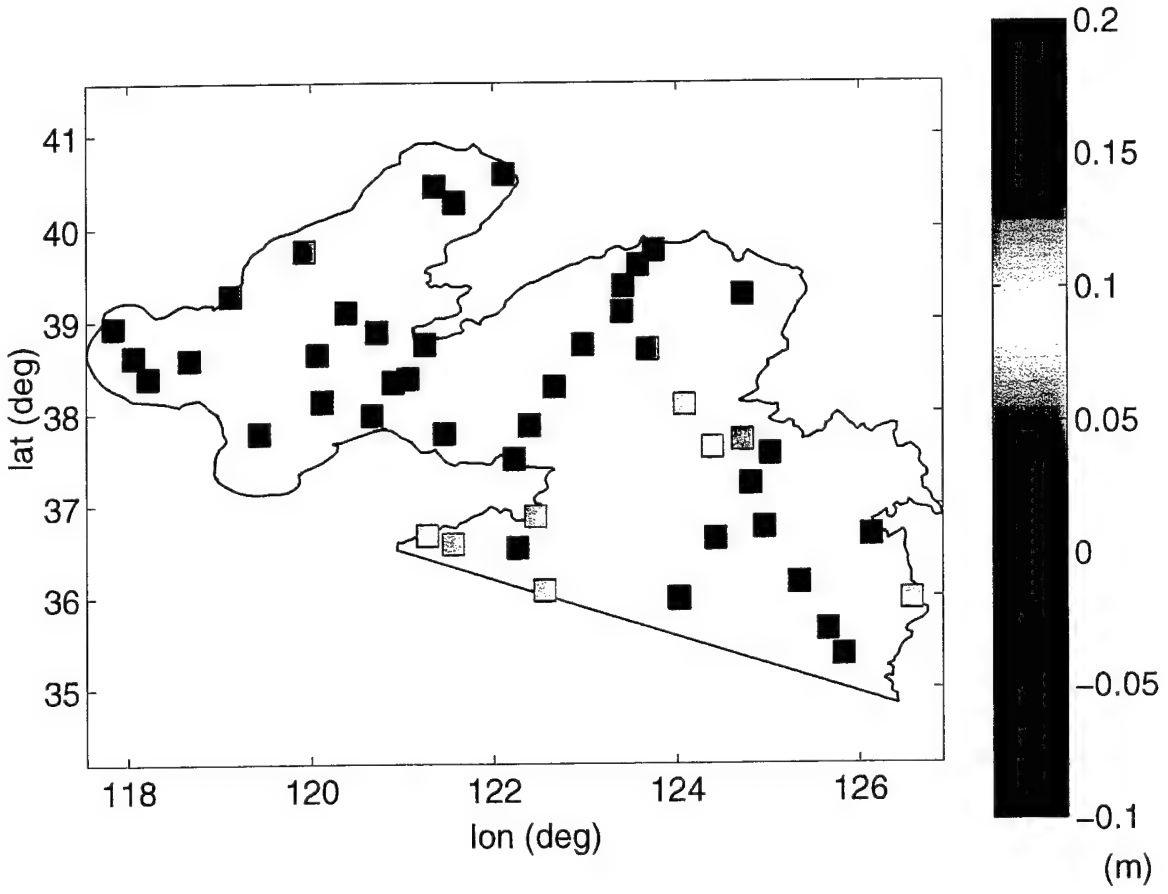

Fig. 16 — Root mean square error by station for the difference between the *subadj2* solution and the "subadj2 i1" solution produced with forcing interpolated from the linear ADJOINT model

grid solutions, the use of open boundary forcing from the linear ADJOINT model improves the solution throughout nearly all of the domain (at the boundary, through the interior, and into the Bohai Sea). Near observation stations, the solution is constrained by the assimilation of data values (Pistek et al. 1998). The improvement in this *subadj2* solution at this particular boundary may be the result of the proximity of the open boundary to many locations where data are assimilated into the linear ADJOINT model.

The results of these three limited area domain experiments demonstrate that the linear ADJOINT model solution is highly dependent upon the observational data assimilated. Three limited area domains having three different open ocean boundary locations result in complex model solutions that are unpredictable with respect to their improvement or degradation in comparison to measured data. The coarse resolution of the ADJOINT model as applied here is a likely cause of this data dependence.

5. CONCLUSIONS

An adjoint model system comprising a dynamically simple model and its inverse in conjunction with a more dynamically complex forward model has been applied in the Yellow Sea to predict tidal elevations and currents throughout the region using the incremental approach. A systematic series of model experiments has shown that the incremental approach diverges for the model configurations employed. Several factors contribute to this result, foremost being incompatibilities between ADCIRC and the Thompson linear ADJOINT model, as configured. The two models solve different model equations, have radically different discrete formulations, widely disparate resolution, and differing open boundary forcing representations. Limited domain modeling using the assimilative model as a source of boundary forcing is also investigated. This approach indicates a strong dependence of the linear ADJOINT model as defined upon the observational data.

One of the primary impedances to success of the incremental approach as applied is the widely disparate resolution of the computational grids used by the complex forward model and the linear ADJOINT model. The complex model ADCIRC is exercised over a mesh with resolution from 4 to 20 km, sufficient to resolve the speed of gravity waves. In contrast, the linear (finite difference) ADJOINT model has a far coarser resolution of 40 km, which is demonstrated to be sufficient for a linear model constrained by assimilated observations (Perkins and Pistek 1998). This coarse resolution is likely insufficient without data assimilation and increases the data dependence of the linear model solution. Furthermore, the differences in resolution create a land/sea boundary mismatch between forward and ADJOINT models that contribute further to divergence of the method. Typical applications of adjoint models using the incremental approach maintain identical resolutions for the forward and inverse models.

Another discrepancy between the ADCIRC and the Thompson model is the theoretical difference in the boundary condition formulations. Using the incremental approach as applied here, the linear ADJOINT model is forced by surface elevations as well as fluxes, and the open boundary condition is radiated about that state imposed at the boundary. By contrast, the complex forward model, ADCIRC, uses specified elevation or specified fluxes along the open boundary. No radiation of energy across the open boundary takes place. In the incremental approach of Thompson et al. (2000), the expression of the boundary forcing is an essential component of the optimization procedure.

Lastly, a known discrepancy at the start of these experiments is the waiver on having a true adjoint for the complex forward model. The ADJOINT model used is not the adjoint of the discrete linear equations of the complex forward model. Both model equations, Generalized Wave Continuity Equation vs primitive Shallow Water equations, and discretizations, finite element vs finite difference, are dissimilar. These incompatibilities are known to be potentially problematic. This work, however, does not prove conclusively that these factors are solely responsible for the failure of the incremental approach. Rather, failure of the incremental approach as applied here can be ascribed to some combination of resolution disparity, incompatible boundary conditions, and differing model formulations.

In another approach, the optimal ADJOINT model solution serves as a source of open boundary forcing for a limited area domain complex forward model external to the data assimilation loop. Improvements in the complex model performance as shown here are unpredictable due to a strong dependence of the ADJOINT model solution on the placement of the open boundary and the observational data assimilated.

It is anticipated that an adjoint model system that is derived from the discrete linear equations associated with the complex forward model would ensure a convergent solution. The forward model specified by ADCIRC and the linear adjoint model system TRUXTON/FUNDY (Lynch et al. 1998; Naimie and Lynch 2000) would be an obvious choice. Compatible boundary conditions would increase the likelihood for successful convergence. Such a model system could be used to further improve understanding of the factors affecting successful implementation of the incremental data assimilative approach. Addition insight into the tidal dynamics and an enhanced ability to forecast tidal elevations in the Yellow Sea are also expected.

6. ACKNOWLEDGMENTS

Gratitude is extended to W.J. Teague for ADCP station data and processing, Hank Perkins, Pavel Pistek, and Jeff Book for their collaboration and discussions, and Keith Thompson and Pavel Pistek for their work with the linear ADJOINT model. This work has been supported through the Space and Naval Warfare Systems Command "Korean Coastal Environment" Program Element 0603207N, under the direction of Dr. Ed Harrison.

REFERENCES

Bennett, A.F., *Inverse Methods in Physical Oceanography* (Cambridge University Press, New York, 1992).

Blain, C.A., J.J. Westerink, and R.A. Luettich, "The Influence of Domain Size on the Response Characteristics of a Hurricane Storm Surge Model," *J. Geophys. Res.* **99**(C9), 18467-18479, 1994.

Book, J., personal communication, 2000.

Courtier, P., J.-N. Thepaut, and A. Hollingsworth, "A Strategy for Operation Implementation of 4D-var, Using an Incremental Approach," *Quart. J. Roy. Met. Soc.* **120**, 1367-1387, 1994.

Ghil, M., K. Ide, A. Bennett, P. Courtier, M. Kimoto, M. Nagata, M. Saiki, and M. Sato (eds.), *Data Assimilation in Meteorology and Oceanography: Theory and Practice* (Meteorological Society of Japan and Universal Academy Press, Tokyo, 1997).

Ghil, M. and P. Manalotte-Rizzoli, "Data Assimilation in Meteorology and Oceanography," *Adv. in Geophys.* **33**, 141-266, 1991.

Griffin, D.A. and K.R. Thompson, "The Adjoint Method of Data Assimilation Used Operationally for Shelf Circulation," *J. Geophys. Res.* **101**(C2), 3457-3477, 1996.

Jacobs, G.A., R.H. Preller, S.K. Riedlinger, and W.J. Teague, "Coastal Wave Generation in the Bohai Bay and Propagation Along the Chinese Coast," *Geophys. Res. Lett.* **25**(6), 777-780, 1998.

Kinnmark, I.P.E., "The Shallow Water Wave Equations: Formulation, Analysis, and Application," Ph.D. dissertation, Dept. of Civil Eng., Princeton Univ., N.J., 1984.

Kolar, R.L., W.G. Gray, J.J. Westerink, and R.A. Luettich, "Shallow Water Modeling in Spherical Coordinates: Equation Formulation, Numerical Implementation, and Application," *J. Hydraul. Res.* **32**, 3-24, 1994a.

Kolar, R.L., J.J. Westerink, M.E. Cantekin, and C.A. Blain, "Aspects of Nonlinear Simulations Using Shallow Water Models Based on the Wave Continuity Equation," *Comput. Fluids* **23**, 523-538, 1994b.

Lardner, R.W., "Optimal Control of Open Boundary Conditions for a Numerical Tidal Model," *Comp. Meth. App. Mech. Eng.* **102**, 367-387, 1993.

Le Provost, C., M.L. Genco, F.H. Lyard, P. Vincent, and P. Canceil, "Tidal Spectroscopy of the World Ocean Tides from a Finite Element Hydrodynamic Model," *J. Geophys. Res.* **99**(C12), 24777-24798, 1994.

LeProvost, C. and P. Vincent, "Some Tests of Precision for a Finite Element Model of Ocean Tides," *J. Comp. Physics* **65**, 273-291, 1986.

Luettich, R.A., J.J. Westerink, and N.W. Scheffner, "ADCIRC: An Advanced Three-dimensional Circulation Model for Shelves, Coasts, and Estuaries, Report 1: Theory and Methodology of ADCIRC-2DDI and ADCIRC-3DL," *Tech. Rep. DRP-92-6*, Dept. of the Army, Washington, D.C., 1992.

Lynch, D.R., "Progress in Hydrodynamic Modeling. Review of U.S. Contributions, 1979-1982," *Rev. Geophys.* **21**(3), 741-754, 1983.

Lynch, D.R. and W.G. Gray, "A Wave Equation Model for Finite Element Tidal Computations," *Comp. Fluids* **7**, 207-228, 1979.

Lynch, D.R., C.E. Naimie, and C.G. Hannah, "Hindcasting the Georges Bank Circulation. Part I: Detiding," *Cont. Shelf Res.* **18**, 607-639, 1998.

Naimie, C.E. and D.R. Lynch, "Inversion Skill for Limited-area Shelf Modeling - Observational System Simulation Experiments," *Cont. Shelf Res.*, in press, 2000.

Perkins, H. and P. Pistek, "Rapid Environmental Assessment by Data Assimilation," Oceanology International '98, *2*, New Malden, Surrey, U.K., 1998.

Pistek, P., H. Perkins, J. Boyd, and K.R. Thompson, "Determining the Coastal Environment by Data Assimilation Using an Adjoint Technique," in *Rapid Environmental Assessment*, Pouliqwuen, E., A.D. Kirman, and R. T. Pearson (eds) (NATO SACLANTCEN, La Spezia, Italy, 1998).

Roed, L.P. and O.M. Smedstad, "Open Boundary Conditions for Forced Waves in a Rotating Fluid," *SIAM J. Sci. Stat. Comp.* **2**, 414-26, 1984.

Seiler, U., "Estimation of Open Boundary Conditions with the Adjoint Method," *J. Geophys. Res.* **98**(22), 855-870, 1993.

Thompson, K.R., M. Dowd, Y. Lu and B. Smith, "Oceanographic Data Assimilation and Regression Analysis," *Environmetrics 2000* **11**, 183-196, 2000.

Thompson, K.R., M. Dowd and Y. Lu, "Oceanographic Data Assimilation from the Perspective of Nonlinear Regression," American Statistical Association, Proceedings, 1998.

Thompson, K.R. and D.A. Griffin, "A Model of the Circulation on the Outer Scotian Shelf with Open Boundary Conditions Inferred by Data Assimilation," *J. Geophys. Res.* **103**(C13), 30641-30660, 1998.

Westerink, J.J., C.A. Blain, R.A. Luettich, and N.W. Scheffner, "ADCIRC: An Advanced Three-dimensional Circulation Model for Shelves, Coasts, and Estuaries, Report 2: User's Manual for ADCIRC-2DDI," *Tech. Rep. DRP-92-6*, Dept. of the Army, Washington, D.C., 1994a. http://www.marine.unc.edu/C_CATS/adcirc/document/ADCIRC_main_frame.html

Westerink, J.J., R.A. Luettich, and J.C. Muccino, "Modeling Tides in the Western North Atlantic Using Unstructured Graded Grids," *Tellus*, **46A** 187-199, 1994b.

Westerink, J.J., R.A. Luettich, and S.C. Hagen, "Meshing Requirements of Large Scale Coastal Ocean Tidal Models," in *Numerical Methods in Water Resources*, A. Peters, G. Wittum, B. Herrling, and U. Meissner (eds.) (Kluwer Academic Publishers, The Netherlands, 1994c).

Westerink, J.J. and W.G. Gray, "Progress in Surface Water Modeling," *Rev. Geophys.* **29**, Suppl., 210-217, 1991.